



## Comparisons between azo dyes and Schiff bases having the same benzothiazole/phenol skeleton: Syntheses, crystal structures and spectroscopic properties

Tao Tao, Feng Xu, Xiao-Chun Chen, Qian-Qian Liu, Wei Huang\*, Xiao-Zeng You

State Key Laboratory of Coordination Chemistry, Nanjing National Laboratory of Microstructures, School of Chemistry and Chemical Engineering, Nanjing University, Nanjing 210093, PR China

### ARTICLE INFO

#### Article history:

Received 5 July 2011

Received in revised form

9 September 2011

Accepted 12 September 2011

Available online 17 September 2011

#### Keywords:

Benzothiazole

Azo dyes

Schiff bases

Electronic spectra

Crystal structures

$\pi$ - $\pi$  Stacking interactions

### ABSTRACT

Three pairs of heterocyclic azo dyes and their corresponding Schiff bases were prepared by diazotization and Schiff-base condensation reactions between substituted 2-aminobenzothiazoles and either 3-(diethylamino)phenol or 3,5-dichloro-2-hydroxybenzaldehyde in order to obtain some high performance Disperse Red dyes and compare the structural and spectral differences between the azo dyes and Schiff bases. All azo dyes and Schiff bases in this work have the same benzothiazole/phenol skeleton but different substituent group in the phenyl ring. X-ray single-crystal diffraction analyses of selected compounds reveal that they have a similar planar conformation between the benzothiazole and phenol units but dissimilar dimeric crystal packing. Electronic spectra of the dyes demonstrate that the presence of N=N and C=N double bond chromophore units as well as substituent effects of different auxochrome groups in the benzothiazole backbone leads to significant alterations of bathochromic and hypsochromic shifts despite only slight differences in their molecular structures.

© 2011 Elsevier Ltd. All rights reserved.

### 1. Introduction

Azo-functionalized dyes bearing aromatic heterocyclic components [1] have attracted ever increasing attention in recent years because of their wide applications in metallochromic indicators [2], optical data storage [3], non-linear optics [4], and dye-sensitized solar cells [5]. Specifically, aromatic azo derivatives containing intramolecular D- $\pi$ -A charge-transfer chromophores show excellent photo-physical properties [6–8] since they have extensive  $\pi$ -systems delocalized between the acceptor and donor units across the azo linkage.

It is also known that amino groups can react reversibly with aldehyde groups to form Schiff bases having conjugated carbon-nitrogen double bonds. Comparisons between the nitrogen-nitrogen double bonds in azo dyes with the carbon-nitrogen double bonds in Schiff bases appear to be quite interesting from structures to related properties. On the one hand, electronic spectra of azo dyes show that they have maximum absorptions ( $\lambda_{\max}$ ) at red or near infrared wavelengths with extraordinarily large molar absorption coefficient ( $\xi$ )

because of the low band gap of  $\pi$ - $\pi^*$  transition in azo dye systems. On the other hand, molecular conformation and packing fashion of these two kinds of compounds in the solid state and in the bulk, which may be influenced by the supra-molecular interactions among molecules, are of great significance and worth discussing [9–12].

In our previous work, several Disperse Yellow azo dyes crystallizing in the hydrazone form in the solid state and their azo-hydrazone tautomerisms have been investigated [13–17]. At the same time, we have studied four heterocyclic Disperse Red azo dyes having the same benzothiazole/azo/benzene skeleton in crystallographic terms [18]. As an extensive study in this area, we report herein three pairs of heterocyclic azo dyes and their corresponding Schiff bases **1–6** bearing the same benzothiazole/phenol skeleton. Among them, single-crystal structures of compounds **2** and **5** are included for comparison. They have an electron-donating methyl group (**1** and **4**) or an electron-withdrawing nitro group (**3** and **6**) as well as an electron-donating *p*-positioned diethylamino unit (**1–3**) or an electron-withdrawing dichloro unit (**4–6**) in their molecular structures. The aim of combing various donor-acceptor substituents is to finely tune their electronic structures and compare the spectroscopic properties between azo dyes and Schiff bases bearing similar aromatic moieties linked by nitrogen-nitrogen and carbon-nitrogen double bonds.

\* Corresponding author. Tel.: +86 25 83686526; fax: +86 25 83314502.  
E-mail address: [whuang@nju.edu.cn](mailto:whuang@nju.edu.cn) (W. Huang).

## 2. Experimental section

### 2.1. Materials and measurements

All melting points were measured without correction. The reagents of analytical grade were purchased from commercial sources and used without any further purification. Elemental analyses (EA) for carbon, hydrogen, and nitrogen were performed on a Perkin–Elmer 1400C analyzer. Infrared (IR) spectra (4000–400  $\text{cm}^{-1}$ ) were recorded using a Nicolet FT–IR 170X spectrophotometer on KBr disks. Electrospray ionization mass spectra (ESI–TOF–MS) were recorded on a Finnigan MAT SSQ 710 mass spectrometer in a scan range of 200–2000 amu. Electro-ionization mass spectra (EI–TOF–MS, electron energy 70 eV) were recorded by GCT TOF mass spectrometry (Micromass, Manchester, UK).  $^1\text{H}$  NMR spectra were measured with a Bruker DMX500 MHz NMR spectrometer at room temperature in  $\text{CDCl}_3$  with tetramethylsilane as the internal reference. UV–Vis spectra were recorded with a Shimadzu UV-3150 double-beam spectrophotometer using a Pyrex cell with a path length of 10 mm.

### 2.2. Synthesis

#### 2.2.1. 5-(Diethylamino)-2-((6-methylbenzo[d]thiazol-2-yl)diazanyl)phenol (**1**)

2-Amino-6-methylbenzothiazole (1.64 g, 10.0 mmol) was dissolved in a mixture of concentrated sulfuric acid (2 mL) and glacial acetic acid (10 mL) at  $-5^\circ\text{C}$  in an ice bath. Sodium nitrite (0.76 g, 11.0 mmol) was dissolved in cold water and added dropwise to the reaction mixture for 0.5 h under stirring. The diazonium salt was obtained and used for the next coupling reaction. 3-(Diethylamino)phenol (1.65 g, 10.0 mmol) was added to a mixture of methanol/water (90 mL, 2:1, v/v) solution in a three-necked flask immersed in an ice bath. Freshly prepared diazonium salt was added dropwise for 1 h to the reaction mixture under vigorous mechanical stirring ( $0-5^\circ\text{C}$ ). After additional stirring for 1.5 h, the mixture was neutralized with aqueous ammonia to pH 5–6 for 0.5 h. The precipitate was filtered and dried after thorough washing with acetone and ethanol. The crude product was recrystallized and microcrystals of **1** were obtained. Further purification was performed by column chromatography using  $\text{CHCl}_3$  as eluent. Yield, 2.67 g (79%), m.p.  $232-234^\circ\text{C}$ ;  $^1\text{H}$  NMR (500 MHz,  $\text{CDCl}_3$ , ppm):  $\delta$  13.61 (s, 1H, OH), 7.84 (d, 1H, benzo), 7.60 (s, 1H, benzo), 7.53 (d, 1H, phenol), 7.24 (d, 1H, benzo), 6.46 (dd, 1H, phenol), 6.14 (d, 1H, phenol), 3.48 (q, 4H,  $\text{CH}_2$ ), 2.48 (s, 3H,  $\text{CH}_3$ -benzo), and 1.27 (t, 6H,  $\text{CH}_3$ ); Main FT–IR absorptions (KBr pellets,  $\nu$ ,  $\text{cm}^{-1}$ ): 3405 (vs), 2975 (w), 1629 (m), 1527 (w), 1135 (vs), 817 (w), 639 (m), and 618 (m). ESI–TOF–MS (positive):  $m/z$  341.2  $[\text{M} + \text{H}]^+$ , 363.1  $[\text{M} + \text{Na}]^+$ ; Elemental analysis: calcd (%) for  $\text{C}_{18}\text{H}_{20}\text{N}_4\text{O}_2$ : C, 63.50; H, 5.92; N, 16.46; found: C, 63.72; H, 5.99; N, 16.23.

#### 2.2.2. 2-(Benzo[d]thiazol-2-yl)diazanyl-5-(diethylamino)phenol (**2**) and 5-(diethylamino)-2-((6-nitrobenzo[d]thiazol-2-yl)diazanyl)phenol (**3**)

The syntheses of compounds **2** and **3** were similar to that described for compound **1**. Compound **2**: Yield, 2.41 g (74%), m.p.  $228-229^\circ\text{C}$ ;  $^1\text{H}$  NMR (500 MHz,  $\text{CDCl}_3$ , ppm):  $\delta$  13.65 (s, 1H, OH), 7.89 (d, 1H, benzo), 7.73 (d, 1H, benzo), 7.46 (d, 1H, phenol), 7.36 (t, 1H, benzo), 7.20 (t, 1H, benzo), 6.40 (dd, 1H, phenol), 6.07 (d, 1H, phenol), 3.42 (q, 4H,  $\text{CH}_2$ ), and 1.20 (t, 6H,  $\text{CH}_3$ ); Main FT–IR absorptions (KBr pellets,  $\nu$ ,  $\text{cm}^{-1}$ ): 3400 (vs), 1632 (m), 1408 (s), 1111 (vs), and 617 (m). ESI–TOF–MS: (positive)  $m/z$  327.2  $[\text{M} + \text{H}]^+$ , 349.2  $[\text{M} + \text{Na}]^+$ ; Elemental analysis: calcd (%) for  $\text{C}_{17}\text{H}_{18}\text{N}_4\text{O}_2$ : C, 62.55; H, 5.56; N, 17.16; found: C, 62.71; H, 5.79; N, 16.98. Compound **3**: Yield, 2.67 g (72%), m.p.  $287-289^\circ\text{C}$ ;  $^1\text{H}$  NMR

(500 MHz,  $\text{CDCl}_3$ , ppm):  $\delta$  14.05 (s, 1H, OH), 8.70 (d, 1H, benzo), 8.28 (s, 1H, benzo), 7.96 (d, 1H, benzo), 7.50 (d, 1H, phenol), 6.54 (dd, 1H, phenol), 6.13 (d, 1H, phenol), 3.53 (q, 4H,  $\text{CH}_2$ ), and 1.25 (t, 6H,  $\text{CH}_3$ ); Main FT–IR absorptions (KBr pellets,  $\nu$ ,  $\text{cm}^{-1}$ ): 3410 (vs), 1640 (m), 1527 (m), 1332 (m), 1297 (m), 1124 (s), and 617 (m). ESI–TOF–MS (positive):  $m/z$  372.2  $[\text{M} + \text{H}]^+$ , 395.1  $[\text{M} + \text{Na}]^+$ ; Elemental analysis: calcd (%) for  $\text{C}_{17}\text{H}_{17}\text{N}_5\text{O}_3\text{S}$ : C, 54.97; H, 4.61; N, 18.86; found: C, 55.11; H, 4.77; N, 18.56.

#### 2.2.3. 2,4-Dichloro-6-((6-methylbenzo[d]thiazol-2-ylimino)methyl)phenol (**4**)

About 10 g of 4 Å molecular sieves were added into a toluene solution (30 mL) of 2-amino-6-methylbenzothiazole (0.50 g, 3.0 mmol) and 3,5-dichloro-2-hydroxybenzaldehyde (0.57 g, 3.0 mmol), and the reaction mixture was heated under reflux for 24 h with vigorous mechanical agitation. The mixture was then filtered from the molecular sieves which were washed with solvent. The solvent was removed from the filtrate and washings by rotary evaporation, and the product purified by either vacuum distillation or crystallization. Yield, 0.89 g (88%), m.p.  $193-195^\circ\text{C}$ ;  $^1\text{H}$  NMR (500 MHz,  $\text{CDCl}_3$ , ppm):  $\delta$  13.02 (s, 1H, OH), 9.25 (s, 1H,  $\text{CH}=\text{N}$ ), 7.87 (d, 1H, benzo), 7.66 (s, 1H, benzo), 7.54 (d, 1H, phenol), 7.42 (d, 1H, phenol), 7.33 (d, 1H, benzo), and 2.51 (s, 3H,  $\text{CH}_3$ ); Main FT–IR absorptions (KBr pellets,  $\nu$ ,  $\text{cm}^{-1}$ ): 3415 (s), 1650 (m), 1588 (s), 1557 (m), 1481 (m), 1448 (s), 1379 (m), 1354 (m), 1280 (m), 1225 (s), 1184 (s), 1154 (vs), 1099 (s), 862 (m), 808 (m), 775 (m), 742 (m), 681 (m), 564 (w), 465 (w), and 437 (w). EI–TOF–MS:  $m/z$  335.9, 337.9, 340.0  $[\text{M}]^+$ ; Elemental analysis: calcd (%) for  $\text{C}_{15}\text{H}_{10}\text{Cl}_2\text{N}_2\text{O}_2\text{S}$ : C, 53.42; H, 2.99; N, 8.31; found: C, 53.58; H, 3.11; N, 8.56.

#### 2.2.4. 2-((Benzo[d]thiazol-2-ylimino)methyl)-4,6-dichlorophenol (**5**) and 2,4-dichloro-6-((6-nitrobenzo[d]thiazol-2-ylimino)methyl)phenol (**6**)

The syntheses of compounds **5** and **6** were similar to that described for compound **4**. Compound **5**: Yield, 0.82 g (85%), m.p.  $186-188^\circ\text{C}$ ;  $^1\text{H}$  NMR (500 MHz,  $\text{CDCl}_3$ , ppm):  $\delta$  13.00 (s, 1H, OH), 9.28 (s, 1H,  $\text{CH}=\text{N}$ ), 7.99 (d, 1H, benzo), 7.87 (d, 1H, benzo), 7.55 (s, 1H, phenol), 7.53 (t, 1H, benzo), 7.43 (s, 1H, phenol), and 7.42 (t, 1H, benzo); Main FT–IR absorptions (KBr pellets,  $\nu$ ,  $\text{cm}^{-1}$ ): 3418 (vs), 2360 (w), 1646 (m), 1596 (s), 1558 (m), 1481 (m), 1434 (s), 1358 (m), 1295 (m), 1191 (m), 1166 (s), 1152 (s), 1102 (m), 874 (m), 806 (w), 753 (s), 742 (m), 725 (m), 680 (m), 626 (w), 563 (w), and 434 (w). EI–TOF–MS:  $m/z$  321.9, 323.9, 326.0  $[\text{M}]^+$ ; Elemental analysis: calcd (%) for  $\text{C}_{14}\text{H}_8\text{Cl}_2\text{N}_2\text{O}_2\text{S}$ : C, 52.03; H, 2.49; N, 8.67; Found: C, 52.21; H, 2.56; N, 8.54. Compound **6**: Yield, 0.81 g (74%), m.p.  $244-246^\circ\text{C}$ ;  $^1\text{H}$  NMR (500 MHz,  $\text{CDCl}_3$ , ppm):  $\delta$  9.35 (s, 1H,  $\text{CH}=\text{N}$ ), 8.83 (s, 1H, benzo), 8.40 (d, 1H, benzo), 8.08 (d, 1H, benzo), 7.62 (s, 1H, phenol), and 7.50 (s, 1H, phenol); Main FT–IR absorptions (KBr pellets,  $\nu$ ,  $\text{cm}^{-1}$ ): 3396 (vs), 1647 (s), 1570 (m), 1526 (s), 1496 (s), 1448 (s), 1327 (s), 1294 (vs), 1206 (m), 1158 (m), 1124 (s), 885 (w), 825 (w), 752 (m), 553 (w), and 432 (w). ESI–TOF–MS (negative):  $m/z$  366.2, 368.1, 370.0  $[\text{M}-\text{H}]^-$ ; Elemental analysis: calcd (%) for  $\text{C}_{14}\text{H}_8\text{Cl}_2\text{N}_2\text{O}_2\text{S}$ : C, 52.03; H, 2.49; N, 8.67; Found: C, 52.21; H, 2.56; N, 8.54.

### 2.3. X-ray data collection and solution

Single-crystal samples of **2** and **5** were glue-covered and mounted on glass fibers for data collection on a Bruker SMART 1K CCD area detector at 191 and 293 K, respectively, using graphite mono-chromated Mo K $\alpha$  radiation ( $\lambda = 0.71073 \text{ \AA}$ ). The collected data were reduced by using the program SAINT [19] and empirical absorption corrections were done by SADABS [20] program. The crystal systems were determined by Laue symmetry and the space groups were assigned on the basis of systematic absences by using

XPREF. The structures were solved by direct method and refined by least-squares method. All non-hydrogen atoms were refined on  $F^2$  by full-matrix least-squares procedure using anisotropic displacement parameters, while hydrogen atoms were inserted in the calculated positions assigned fixed isotropic thermal parameters at 1.2 times of the equivalent isotropic  $U$  of the atoms to which they are attached (1.5 times for the methyl groups) and allowed to ride on their respective parent atoms. In compound **2**, atoms C7 and S1 of the thiazole ring and atom O1 of phenyl ring are refined disorderedly over two positions by the free variable method and the final site occupancy factors are given as 0.651(3) and 0.349(3), respectively. All calculations were carried out using the SHELXTL PC program package [21] and molecular graphics were drawn by using XSELL, XP and ChemDraw softwares. Details of the data collection and refinement results for compounds **2** and **5** are listed in Table 1, while selected bond distances and bond angles are given in Table 2.

#### 2.4. Computational details

All calculations were carried out with Gaussian03 programs [22]. The geometries of **1–6** were fully optimized and calculated by B3LYP method and 6-31G\* basis set without any symmetry constraints. The single-crystal structures of **2** and **5** were used as the starting geometries, while other input files were obtained by the substituent-modified approach based on earlier output files.

### 3. Results and discussion

#### 3.1. Syntheses

Azo dyes **1–3** having the same benzothiazole/phenol skeleton were prepared via classical diazotization reactions between 3-(diethylamino)phenol and the corresponding diazonium salts, while Schiff bases **4–6** were synthesized by the formation of the carbon–nitrogen double bond between substitutional 2-amino-benzothiazole compounds and 3,5-dichloro-2-hydroxybenzaldehyde using dehydration condensation reactions (Scheme 1).

**Table 1**  
Crystal data and structural refinements for compounds **2** and **5**.

Compound	<b>2</b>	<b>5</b>
Empirical formula	C <sub>17</sub> H <sub>17</sub> N <sub>4</sub> O <sub>5</sub>	C <sub>14</sub> H <sub>8</sub> Cl <sub>2</sub> N <sub>2</sub> O <sub>5</sub>
Formula weight	325.42	323.19
Temperature/K	191	293
Wavelength/Å	0.71073	0.71073
Crystal size (mm)	0.10 × 0.11 × 0.12	0.30 × 0.25 × 0.20
Crystal system	Monoclinic	Monoclinic
Space group	<i>P</i> 2 <sub>1</sub> / <i>c</i>	<i>P</i> 2 <sub>1</sub> / <i>c</i>
<i>a</i> /Å	7.114(2)	11.841(3)
<i>b</i> /Å	20.770(6)	8.046(2)
<i>c</i> /Å	12.721(4)	14.454(3)
$\alpha$ /°	90	90
$\beta$ /°	122.263(4)	102.613(3)
$\gamma$ /°	90	90
<i>V</i> /Å <sup>3</sup>	1589.4(8)	1343.8(5)
<i>Z</i> / <i>D</i> <sub>calcd</sub> (g/cm <sup>3</sup> )	4/1.360	4/1.597
<i>F</i> (000)	684	656
$\mu$ /mm <sup>-1</sup>	0.214	0.633
<i>h</i> <sub>min</sub> / <i>h</i> <sub>max</sub>	−8/8	−15/11
<i>k</i> <sub>min</sub> / <i>k</i> <sub>max</sub>	−22/24	−10/10
<i>l</i> <sub>min</sub> / <i>l</i> <sub>max</sub>	−15/13	−18/18
Data/parameters	2796/250	3223/182
Final <i>R</i> indices [ <i>I</i> > 2 $\sigma$ ( <i>I</i> )]	<i>R</i> 1 = 0.0452 <i>wR</i> 2 = 0.1216	<i>R</i> 1 = 0.0397 <i>wR</i> 2 = 0.1041
<i>R</i> indices (all data)	<i>R</i> 1 = 0.0578 <i>wR</i> 2 = 0.1278	<i>R</i> 1 = 0.0549 <i>wR</i> 2 = 0.1122
<i>S</i>	1.081	0.994
Max./min. $\Delta\rho$ /e Å <sup>-3</sup>	0.47/−0.49	0.34/−0.26

**Table 2**  
Selected bond distances (Å) and angles (°) for compounds **2** and **5**.

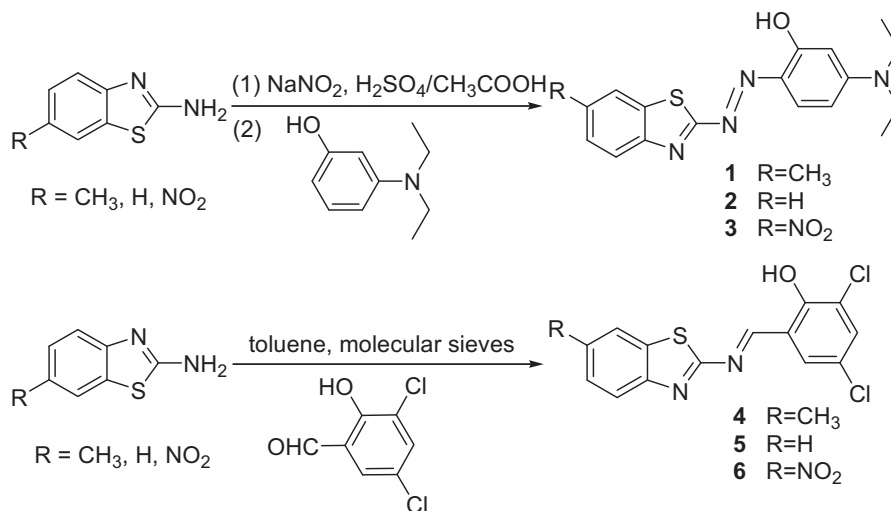
Bond distances		Bond angles	
<b>2</b>			
S1–C5	1.709(3)	C5–S1–C7	89.2(2)
S1–C7	1.768(7)	C6–S1–C7'	92.3(4)
S1'–C6	1.705(6)	C6–N1–C7	104.5(8)
S1'–C7'	1.737(13)	C5–N1'–C7'	107.3(11)
O1–C9	1.296(4)	N3–N2–C7	116.8(5)
O1'–C13	1.208(6)	N3–N2'–C7'	123.9(8)
N1–C6	1.431(10)	N2–N3–C8	123.6(4)
N1–C7	1.325(14)	N2'–N3–C8	144.4(6)
N1'–C5	1.403(14)	C14–N4–C16	116.4(2)
N1'–C7'	1.347(14)	C11–N4–C16	121.0(3)
N2–N3	1.147(6)	C11–N4–C14	122.2(2)
N2–C7	1.406(5)	N1'–C5–C4	120.2(6)
N2'–N3	0.980(7)	S1–C5–C4	130.5(3)
N2'–C7'	1.366(10)	N1'–C5–C6	119.0(6)
N3–C8	1.356(4)	S1–C5–C6	108.7(2)
N4–C14	1.469(5)	N1–C6–C5	119.0(5)
N4–C11	1.357(3)	S1'–C6–C1	132.9(4)
N4–C16	1.468(4)	S1'–C6–C5	106.8(3)
		S1–C7–N2	120.1(5)
<b>5</b>			
Cl1–C11	1.737(2)	C5–S1–C7	88.7(1)
Cl2–C13	1.727(2)	C6–N1–C7	109.8(2)
S1–C5	1.725(2)	C7–N2–C8	117.4(2)
S1–C7	1.734(2)	S1–C5–C4	129.1(2)
O1–C14	1.340(2)	S1–C5–C6	109.5(1)
N1–C6	1.391(2)	N1–C6–C5	114.8(2)
N1–C7	1.296(2)	N1–C6–C1	125.6(2)
N2–C7	1.401(2)	S1–C7–N2	117.0(1)
N2–C8	1.278(2)	N1–C7–N2	126.0(2)
C8–C9	1.441(3)	S1–C7–N1	117.0(1)
		N2–C8–C9	122.7(2)
		Cl1–C11–C10	120.0(2)
		Cl1–C11–C12	119.1(1)
		Cl2–C13–C12	118.9(1)
		Cl2–C13–C14	119.5(1)
		O1–C14–C13	118.9(2)
		O1–C14–C9	122.4(2)

Concentrated sulfuric acid and glacial acetic acid system was used as the reaction mediator in the synthetic process of azo dyes because of the low solubility of substitutional 2-aminobenzothiazole compounds. Molecular sieves 4 Å were added as the catalyst in the synthetic process of Schiff bases due to low reactivity of the aromatic amine components.

All three pairs of compounds **1–6** were fully characterized by <sup>1</sup>H NMR, FT–IR UV–Vis, TOF–MS and elemental analyses. The assignments of <sup>1</sup>H NMR peaks of aromatic heterocyclic compounds **1–6** show the sequence of deshielding effects for the substituent groups as: nitro > hydrogen > methyl. As can be seen in Scheme 2, the chemical shifts ( $\delta$ ) of hydrogen atoms of benzothiazole and phenol rings resonate in the range 6.14–7.88 ppm. However, the assignments of different protons of compounds **1** and **4** can be analyzed by means of the deshielding effects and the splitting of signals. More importantly, the coupling constant (*J*) analyses reveal that the *J* values of protons of benzene ring from benzothiazole are larger than those of the phenol ring, which can help us to further confirm the final peak assignments. Additionally, X-ray single-crystal diffraction method has been used for characterizing the structures of representative compounds **2** and **5**.

#### 3.2. Structural description of compound **2**

The molecular structure of **2** with atom-numbering scheme is shown in Fig. 1a. It crystallizes in the monoclinic *P*2<sub>1</sub>/*c* space group without the presence of any solvent molecule. The bond length of the azo unit (N2–N3) is 1.147(6) Å, indicative of the typical double-

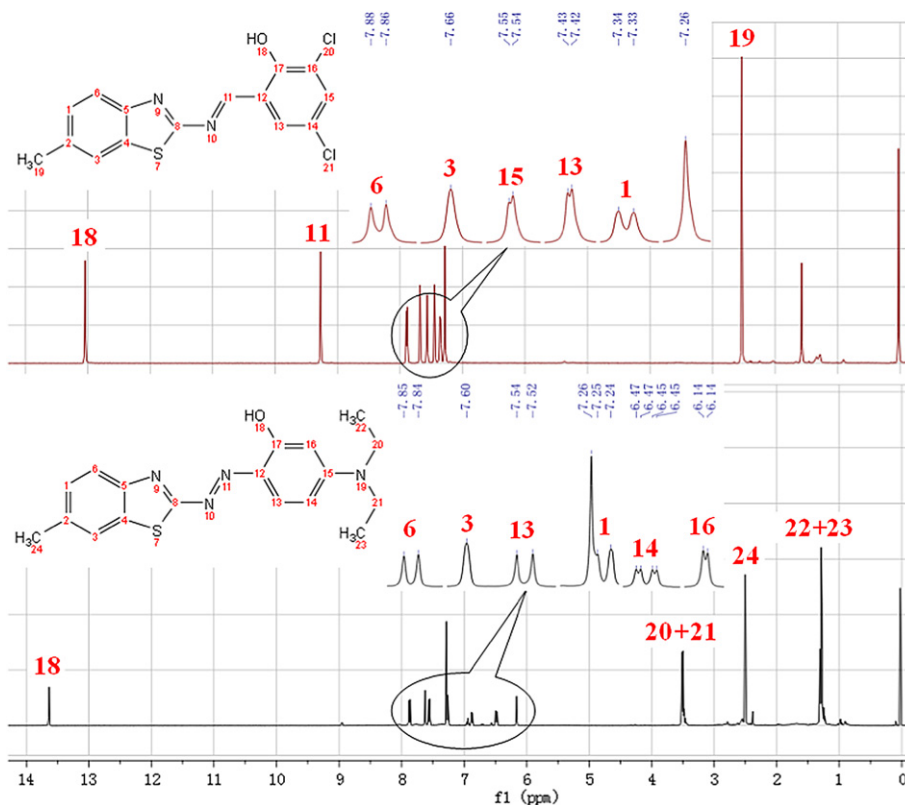


**Scheme 1.** Schematic illustration for the preparation of compounds 1–6.

bond character. In contrast, the N1–C7 bond length is 1.325(14) Å which is shorter than those of N1–C6, N2–C7 and N3–C8 in the lengths of 1.431(10), 1.406(5) and 1.356(4) Å, exhibiting predominantly  $\pi$ -conjugated double-bond character. It is worthwhile to mention that strong intramolecular O–H $\cdots$ N hydrogen bonding interactions are found with the H $\cdots$ A distances of 1.82 and 1.87 Å in **2** forming six-membered C<sub>2</sub>N<sub>2</sub>OH hydrogen bonded rings (Table 3). The thiazole sulfur atom and the azo unit lie at the same side of N2–C7 single bond with the related bond angles of S1–C7–N2 (120.1(5)°), N1–C7–N2 (121.3(7)°), C7–N2–N3 (116.8(5)°) and N2–N3–C8 (123.6(4)°) which are consistent with previously

reported methyl or methoxy substituted benzothiazole azo dyes [18,23,24]. The torsion angles for S1–C7–N2–N3 (3.4(5)°), N1–C7–N2–N3 (176.6(6)°), N2–N3–C8–C9 (2.2(5)°), N2–N3–C8–C13 (177.2(3)°), and C7–N2–N3–C8 (178.8(3)°) exhibit that all the 16 non-hydrogen atoms in the chromophore skeleton, except the *N*-substituted ethyl groups, are essentially coplanar with the mean deviation from least-squares plane of 0.023 Å (Fig. 1b), which is the typical structural feature for most azo dyes.

The *N*-substituted ethyl groups of **2** are found to point to the same side of the above-mentioned molecular least-squares plane,



**Scheme 2.** Schematic illustration for the assignments of <sup>1</sup>H NMR peaks of compounds **1** and **4**.

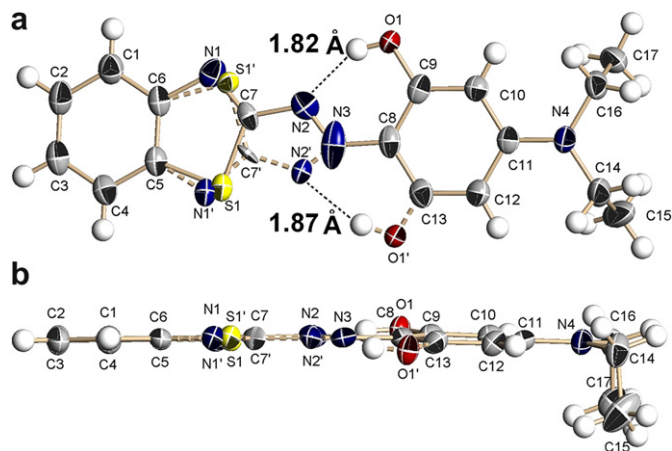


**Fig. 1.** ORTEP drawings of compound **2** with the atom-numbering scheme (top view for **a** and side view for **b**). Displacement ellipsoids are drawn at the 30% probability level and the H atoms are shown as small spheres of arbitrary radii.

which may help to form a head-to-tail dimeric packing mode between adjacent molecules in its crystal structure. As illustrated in Fig. 2,  $\pi$ - $\pi$  stacking interactions are observed between the phenyl rings and the thiazole rings of neighboring molecules with the centroid-to-centroid separation of 3.752 Å, where the alkyl groups point outside of the dimeric units. It is noted that there are two sets of molecules in the crystal packing of **2**, and each set packs in a herringbone fashion and the dihedral angle between them is 86.9°. Furthermore, weak intermolecular C–H...O hydrogen bonding interactions are found between the phenyl hydrogen atom H12 and its adjacent oxygen atom O1.

### 3.3. Structural description of compound **5**

The molecular structure of **5** with atom-numbering scheme is shown in Fig. 3a. It also crystallizes in the monoclinic  $P2_1/c$  space group without the presence of any solvent molecule. The bond length of the imine unit (N2–C8) in **5** is 1.278(2) Å which is a little longer than the N–N azo unit (1.147(6)) Å in **2**, indicative of the difference between nitrogen and carbon atoms. In contrast, the N1–C7 bond length is 1.296(2) Å, which is shorter than those of N1–C6, N2–C7 and C8–C9 in the lengths of 1.391(2), 1.401(2) and 1.441(3) Å too, exhibiting predominantly  $\pi$ -conjugated double-bond character. Intramolecular N–H...O hydrogen bonding interactions are found as well with the H...O distance of 1.93 Å in **5** constituting a six-membered  $C_3NOH$  hydrogen bonded rings. The thiazole nitrogen atom and the imine unit are positioned at the same direction of N2–C7 single bond with the related bond angles of S1–C7–N2 (117.0(1)°), N1–C7–N2 (126.0(2)°), C7–N2–C8 (117.4(2)°) and N2–C8–C9 (122.7(2)°). The torsion angles for

**Table 3**  
Hydrogen bonding parameters (Å, °) in compounds **2** and **5**.

D–H...A	D–H	H...A	D...A	$\angle$ DHA	Symmetry code
<b>2</b>					
O1–H1A...N2	0.82	1.82	2.547(4)	147.0	
O1'–H1A'N2'	0.85	1.87	2.671(8)	156.5	
C12–H12...O1	0.93	2.45	3.240(5)	143.0	1 + x, y, z
<b>5</b>					
O1–H10...N2	0.82	1.93	2.653(2)	146.0	
C8–H8...N1	0.93	2.39	2.753(3)	103.0	

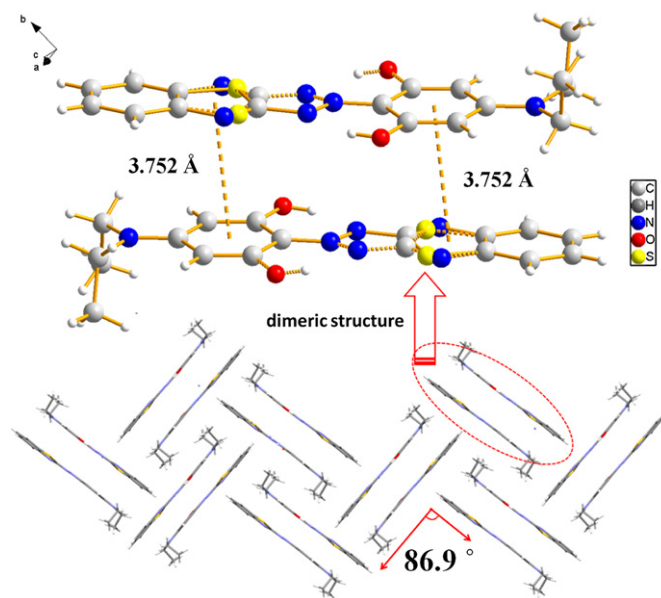


**Fig. 2.** Perspective view and schematic illustration of the packing structures of compound **2**.

S1–C7–N2–C8 (177.6(1)°), N1–C7–N2–C8 (2.1(3)°), N2–C8–C9–C10 (178.2(2)°), N2–C8–C9–C14 (2.3(3)°), and C7–N2–C8–C9 (179.5(2)°) demonstrate that all the 19 non-hydrogen atoms in the chromophore skeleton in **5** are essentially coplanar with the same mean deviation from least-squares plane as that in **2** (Fig. 3b).

In the crystal packing of **5**,  $\pi$ - $\pi$  stacking interactions are observed between the phenyl rings and the benzothiazole rings of contiguous molecules with dissimilar centroid-to-centroid separations of 3.507 and 3.694 Å, respectively (Fig. 4). A head-to-tail dimeric packing fashion between adjacent planar molecules in its crystal structure is also observed. Nevertheless, the aromatic rings between adjacent planar dimeric units are severely offset and no  $\pi$ - $\pi$  stacking interactions can be found in this case, even if there is no steric crowding of alkyl groups and the interlayer separation between them is only 3.298 Å. Additionally, there are also two sets of molecules and each set packs in a herringbone mode and the dihedral angle between them is 67.4°.

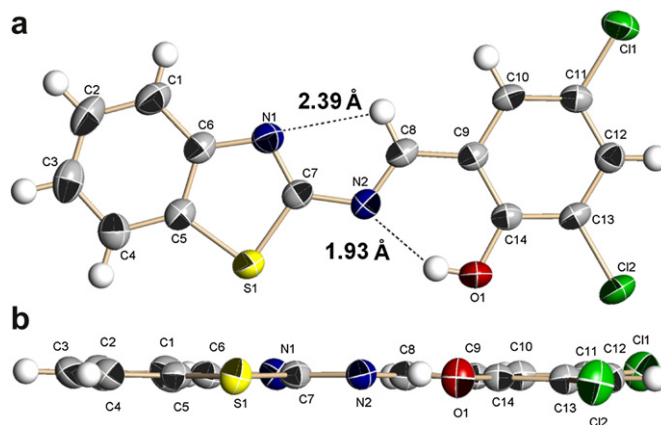


**Fig. 3.** ORTEP drawings of compound **5** with the atom-numbering scheme (top view for **a** and side view for **b**). Displacement ellipsoids are drawn at the 30% probability level and the H atoms are shown as small spheres of arbitrary radii.

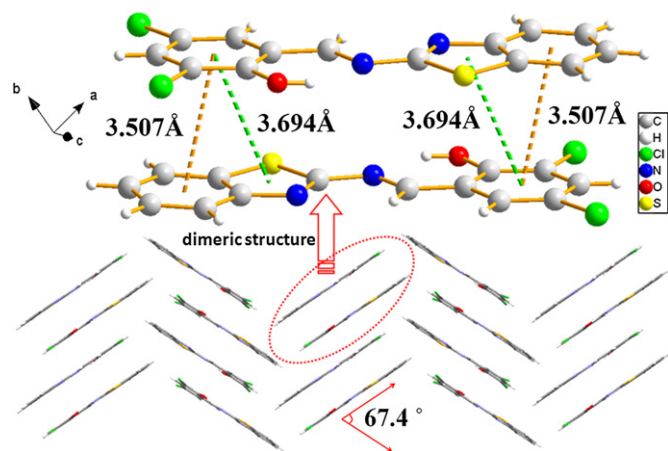


Fig. 4. Perspective view and schematic illustration of the packing structures of compound 5.

#### 3.4. Spectral characterizations and density function theory (DFT) computations

UV–Vis spectra of azo dyes **1–3** and their corresponding Schiff bases **4–6** in their methanol solutions with the same concentration of  $2.0 \times 10^{-5}$  mol/L were recorded at room temperature, respectively, in order to compare the differences originated from their molecular structures. As illustrated in Fig. 5, strong absorption bands at 532, 528, and 538 nm are assigned to the  $\pi-\pi^*$  transition between the aromatic rings and the azo units in compounds **1–3**, which are analogous to our previously reported benzothiazole Disperse Red azo dyes (512–536 nm) [18]. In contrast, the corresponding absorptions of compounds **4–6** shows obvious hypsochromic shifts to 355, 352 and 353 nm because of the presence of different chromophores in their molecular structures ( $-\text{C}=\text{N}-$  versus  $-\text{N}=\text{N}-$  groups), where compound **6** has a very strong absorption peak and the other two are relatively weak. Compared with the absorptions of compounds **2**, the  $\pi-\pi^*$  transition of compound **3** shows a bathochromic shift of 10 nm due to the electron-attracting effects of  $\text{NO}_2$  substituent group. In summary,

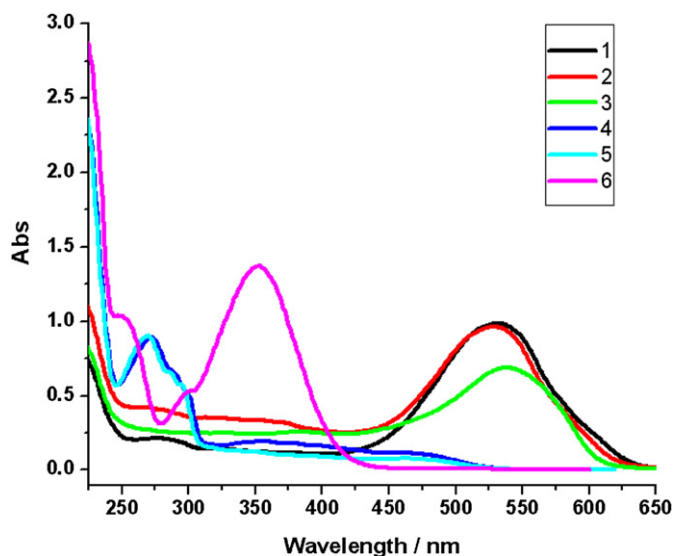


Fig. 5. UV–Vis absorption spectra for azo dyes **1–3** and Schiff bases **4–6** at room temperature in their methanol solutions with the same concentration of  $2.0 \times 10^{-5}$  mol/L.

Table 4

Spectroscopic properties of azo dyes **1–3** and Schiff bases **4–6**. Measurements are made at room temperature in methanol solutions.

Compound	$\lambda_{\text{max}}$ (e) [nm (L mol <sup>-1</sup> cm <sup>-1</sup> )]	$E_{\text{gap}}$ <sup>a</sup> [eV]	$E_{\text{gap}}$ (calcd.) <sup>b</sup> [eV]
<b>1</b>	532 (49600)	2.33	2.91
<b>2</b>	528 (48300)	2.35	2.95
<b>3</b>	538 (34600)	2.30	2.85
<b>4</b>	273 (44700), 355 (9660)	3.49	3.44
<b>5</b>	270 (45200), 352 (6070)	3.52	3.50
<b>6</b>	249 (51700), 353 (68400)	3.51	3.36

<sup>a</sup> Optical band gap determined from the long-wavelength of maximum absorption in the solution UV–Vis spectra.

<sup>b</sup> The geometries of **1–6** were optimized and calculated by B3LYP method and 6-31G\* basis set.

electronic spectral investigations on three pairs of compounds with slight differences in molecular structures demonstrate that the presence of distinguishing azo and Schiff-base units (chromophore groups) as well as substituents (auxochrome groups) in the benzothiazole backbone in **1–6** lead to significant alterations of bathochromic and hypsochromic shifts.

To further reveal the essential distinction of **1–6**, DFT computational studies are carried out where the fixed atom coordinates of compounds **1–6** are used for the highest occupied molecular orbital (HOMO) and the lowest unoccupied molecular orbital (LUMO) gap (band gap) calculations. DFT computational results given in Table 4 reveal that the resultant HOMO–LUMO gaps for azo dyes **1–3** are 2.91, 2.95 and 2.85 eV, respectively, while those for the corresponding Schiff bases **4–6** are much bigger at 3.44, 3.50 and 3.36 eV, respectively, which are in agreement with their UV–vis absorptions. As can be seen in Fig. 6, subtle changes are observed in the calculated spatial representations of HOMOs and LUMOs because of the influences of introducing different electron-donating or electron-withdrawing group in the phenyl ring. Compared with compounds **2** and **5**, introducing an electron-withdrawing nitro group in **3** and **6** is more remarkable than introducing an electron-donating methyl group in **1** and **4**.

Furthermore, not only from the geometry of X-ray diffraction results, but also from that of optimized structures by DFT calculations, the dihedral angles between the benzothiazole and the phenol units are very close to zero showing excellent planarity. In addition to the presence of delocalized  $\pi$  system of molecules, intramolecular hydrogen-bonding and intermolecular  $\pi-\pi$  stacking interactions are believed to play important roles, which are also analogous to those in literature [25]. In addition, the alteration of torsion angles by introducing different substituent groups ( $\text{CH}_3$ , H, or  $\text{NO}_2$ ) in the phenyl ring can be neglected in this case.

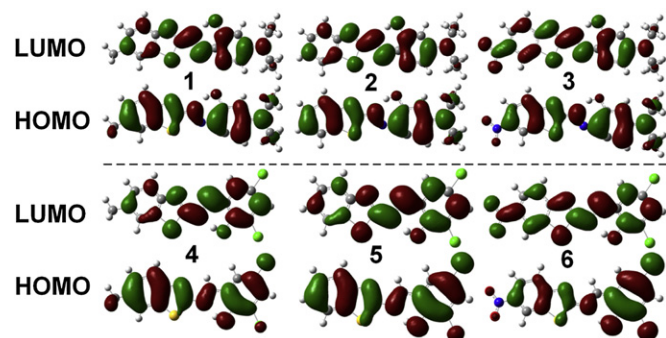


Fig. 6. Calculated spatial representations of HOMOs and LUMOs for azo dyes **1–3** and Schiff bases **4–6** with the DFT B3LYP/6-31(d) level.

#### 4. Conclusion

In summary, three heterocyclic azo dyes and their corresponding Schiff bases having a common benzothiazole/phenol skeleton (**1–6**), have been synthesized and characterized. Comparisons are made between these two types of compounds from syntheses to electronic and molecular structures, spectroscopy and band gaps. X-ray single-crystal diffraction analyses of compounds **2** and **5** reveal that they have similar planar molecular conformation but dissimilar dimeric packing fashions, where two sets of molecules are found and each set packs in a herringbone mode with the dihedral angle of 86.9° and 67.4°, respectively. The spectroscopic properties of **1–6** are dominated by their electronic structures which can be finely tuned by introducing different N=N and C=N double bond units as well as electron-donating and electron-withdrawing groups. Further work is underway on the preparation of azo-functionalized Schiff bases and their transition-metal complexes bearing the same 6-nitrobenzothiazole unit and broad UV–Vis absorption bands, which may be used for fabricating high-efficient dye-sensitized solar cells.

#### Acknowledgements

We acknowledge the Major State Basic Research Development Program (Nos. 2011CB933300, 2007CB925101 and 2011CB808704), the National Natural Science Foundation of China (Nos. 21171088, 21021062 and 20871065) and the Jiangsu Province Department of Science and Technology (No. BK2009226) for financial aids.

#### Appendix. Supplementary material

CCDC reference numbers 831567 and 831568 for compounds **2** and **5** contain the supplementary crystallographic data for this paper. These data can be obtained free of charge at [www.ccdc.cam.ac.uk/conts/retrieving.html](http://www.ccdc.cam.ac.uk/conts/retrieving.html) [or from the Cambridge Crystallographic Data Centre, 12, Union Road, Cambridge CB2 1EZ, UK; Fax: (internat.) +44 1223/336 033; E-mail: [deposit@ccdc.cam.ac.uk](mailto:deposit@ccdc.cam.ac.uk)]. Supplementary data associated with this article can be found in the online version, at doi:10.1016/j.dyepig.2011.09.008.

#### References

- [1] Towns AD. Developments in azo disperse dyes derived from heterocyclic diazo components. *Dyes Pigments* 1999;42(1):3–28.
- [2] Marchevsky E, Olsina R, Marone C. 2-[2-(5-Chloropyridyl)azo]-5-(dimethylamino)phenol as indicator for the complexometric determination of zinc. *Talanta* 1985;32(1):54–6.
- [3] Manickasundaram S, Kannan P, Hassan QMA, Palanisamy PK. Azo dye based poly(alkyloxymethacrylate)s and their spacer effect on optical data storage. *J Mater Sci Mater Electron* 2008;19(11):1045–53.
- [4] Raposo MMM, Fonseca AMC, Castro MCR, Belsley M, Cardoso MFS, Carvalho LM, et al. Synthesis and characterization of novel diazenes bearing pyrrole, thiophene and thiazole heterocycles as efficient photochromic and nonlinear optical (NLO) materials. *Dyes Pigments* 2011;91(1):62–73.
- [5] El Mekki D, Abdel-Mottaleb MSA. The interaction and photostability of some xanthenes and selected azo sensitizing dyes with TiO<sub>2</sub> nanoparticles. *Int J Photoenergy* 2005;7(2):95–101.
- [6] Nosova GI, Abramov IG, Solovskaya NA, Smirnov NN, Zhukova EV, Lyskov VB, et al. Synthesis and photophysical properties of soluble polyimides and polyquinazolones containing side-chain chalcones or azo chromophores. *Polym Sci Ser B* 2011;53(1-2):73–88.
- [7] Razus AC, Birzan L, Cristea M, Tecuceanu V, Blanariu L, Enache C. Novel mono- and bis- azo dyes containing the azulene-1-yl moiety: synthesis, characterization, electronic spectra and basicity. *Dyes Pigments* 2009;80(3):337–42.
- [8] Panda M, Paul ND, Joy S, Hung CH, Goswami S. Hydroxo iridium(III) complexes of azoaromatic ligands: isolation, structure and studies of their physico-chemical properties. *Inorg Chim Acta* 2011;372(1):168–74.
- [9] Leadbetter PW, Leaver AT. Disperse dyes – the challenge of the 1990s. Meeting demands for increasingly higher levels of washfastness in the exhaust dyeing of polyester/cellulosic blends. *Rev Prog Color Relat Top* 1989;19:33–9.
- [10] Fox D, Metrangolo P, Pasini D, Pilati T, Resnati G, Terraneo G. Site-selective supramolecular synthesis of halogen-bonded cocrystals incorporating the photoactive azo group. *Cryst Eng Comm* 2008;10(9):1132–6.
- [11] Lee JE, Kim HJ, Han MR, Lee SY, Jo WJ, Lee SS, et al. Crystal structures of C.I. Disperse Red 65 and C.I. Disperse Red 73. *Dyes Pigments* 2009;80(1):181–6.
- [12] Kennedy AR, Andrikopoulos PC, Arlin JB, Armstrong DR, Duxbury N, Graham DV, et al. Supramolecular structure in s-block metal complexes of sulfonated monoazo dyes: discrepant packing and bonding behavior of ortho-sulfonated azo dyes. *Chem Eur J* 2009;15(37):9494–504.
- [13] Huang W, Qian HF. Structural characterization of C.I. Disperse Yellow 114. *Dyes Pigments* 2008;77(2):446–50.
- [14] Huang W. Structural and computational studies of azo dyes in the hydrazone form having the same pyridine-2,6-dione component (II): C.I. Disperse Yellow 119 and C.I. Disperse Yellow 211. *Dyes Pigments* 2008;79(1):69–75.
- [15] Qian HF, Huang W. An azo dye molecule having a pyridine-2,6-dione backbone. *Acta Crystallogr Sect C Cryst Struct Commun* 2006;62(2):o62–4.
- [16] You W, Zhu HY, Huang W, Hu B, Fan Y, You XZ. The first observation of azohydrazone and *cis-trans* tautomerisms for Disperse Yellow dyes and their nickel(II) and copper(II) complexes. *Dalton Trans* 2010;39:7876–80.
- [17] Hu B, Wang G, You W, Huang W, You XZ. Azo-hydrazone tautomerism by in situ Cu(II) ion catalysis and complexation with the H<sub>2</sub>O<sub>2</sub> oxidant of C.I. Disperse Yellow 79. *Dyes Pigments* 2011;91(2):105–11.
- [18] Geng J, Tao T, Fu SJ, You W, Huang W. Structural investigations on four heterocyclic Disperse Red azo dyes having the same benzothiazole/azo/benzene skeleton. *Dyes Pigments* 2011;90(1):65–70.
- [19] Siemens. SAINT v4 software reference manual. Madison, Wisconsin, USA: Siemens Analytical X-Ray Systems, Inc.; 2000.
- [20] Sheldrick GM. SADABS, program for empirical absorption correction of area detector data. Germany: Univ. of Gottingen; 2000.
- [21] Siemens. SHELXTL, Version 6.10 reference manual. Madison, Wisconsin, USA: Siemens Analytical X-Ray Systems, Inc; 2000.
- [22] Frisch MJ, Trucks GW, Schlegel HB, Scuseria GE, Robb MA, Cheeseman JR, et al. Gaussian 03, revision C.02. Pittsburgh, PA: Gaussian, Inc.; 2004.
- [23] Hökelek T, Seferoğlu Z, Şahin E. 3-[(5,6-Dimethyl-1,3-benzothiazol-2-yl)diazenyl]-1-methyl-2-phenyl-1H-indole. *Acta Crystallogr Sect E Struct Rep Online* 2007;E63(7):o3170.
- [24] Hökelek T, Seferoğlu Z, Şahin E, Kaynak FB. 3-(6-Methoxybenzothiazol-2-yl)diazenyl-1-methyl-2-phenyl-1H-indole. *Acta Crystallogr Sect E Struct Rep Online* 2007;E63(6):o2837–9.
- [25] Kinali S, Demirci S, Calisir Z, Kurt M, Atac ADFT. FT-IR, FT-Raman and NMR studies of 4-(substituted phenylazo)-3,5-diacetamido-1H-pyrazoles. *J Mol Struct* 2011;993:254–8.